

Nonequilibrium spin glass dynamics from picoseconds to 0.1 seconds

F. Belletti,¹ M. Cotallo,² A. Cruz,^{3,2} L.A. Fernandez,^{4,2} A. Gordillo-Guerrero,^{5,2} M. Guidetti,¹ A. Maiorano,^{1,2} F. Mantovani,¹ E. Marinari,⁶ V. Martin-Mayor,^{4,2} A. Muñoz Sudupe,⁴ D. Navarro,⁷ G. Parisi,⁶ S. Perez-Gaviro,² J. J. Ruiz-Lorenzo,^{5,2} S.F. Schifano,¹ D. Sciretti,² A. Tarancon,^{3,2} R. Tripiccione,¹ J.L. Velasco,² and D. Yllanes^{4,2}

¹*Dipartimento di Fisica Università di Ferrara and INFN - Sezione di Ferrara, Ferrara, Italy.*

²*Instituto de Biocomputación y Física de Sistemas Complejos (BIFI), Zaragoza, Spain.*

³*Departamento de Física Teórica, Universidad de Zaragoza, 50009 Zaragoza, Spain.*

⁴*Departamento de Física Teórica I, Universidad Complutense, 28040 Madrid, Spain.*

⁵*Departamento de Física, Universidad de Extremadura, 06071 Badajoz, Spain.*

⁶*Dipartimento di Fisica, INFN and INFN, Università di Roma "La Sapienza", 00185 Roma, Italy.*

⁷*Departamento de Ingeniería, Electrónica y Comunicaciones and Instituto de Investigación en Ingeniería de Aragón, Universidad de Zaragoza, 50018 Zaragoza, Spain.*

(Dated: August 15, 2021)

We study numerically the nonequilibrium dynamics of the Ising Spin Glass, for a time that spans eleven orders of magnitude, thus approaching the experimentally relevant scale (i.e. *seconds*). We introduce novel analysis techniques that allow to compute the coherence length in a model-independent way. Besides, we present strong evidence for a replicon correlator and for overlap equivalence. The emerging picture is compatible with non-coarsening behavior.

PACS numbers: 75.50.Lk, 75.40.Gb, 75.40.Mg

Spin Glasses[1] (SG) exhibit remarkable features, including slow dynamics and a complex space of states: their understanding is a key problem in condensed-matter physics that enjoys a paradigmatic status because of its many applications to glassy behavior, optimization, biology, financial markets, social dynamics.

Experiments on Spin Glasses[1, 2] focus on nonequilibrium dynamics. In the simplest experimental protocol, isothermal aging hereafter, the SG is cooled as fast as possible to the working temperature below the critical one, $T < T_c$. It is let to equilibrate for a *waiting time*, t_w . Its properties are probed at a later time, $t + t_w$. The thermoremanent magnetization is found to be a function of t/t_w , for $10^{-3} < t/t_w < 10$ and t_w in the range 50 s — 10^4 s[3] (see, however,[4]). This lack of any characteristic time scale is named *Full-Aging*. Also the growing size of the coherent domains, the coherence-length, ξ , can be measured[5, 6]. Two features emerge: (i) the lower T is, the slower the growth of $\xi(t_w)$ and (ii) $\xi \sim 100$ lattice spacings, even for $T \sim T_c$ and $t_w \sim 10^4$ s[5].

The sluggish dynamics arises from a thermodynamic transition at T_c [7, 8, 9]. There is a sustained theoretical controversy on the properties of the (unreachable in human times) equilibrium low temperature SG phase, which is nevertheless relevant to (basically nonequilibrium) experiments[10]. The main scenarios are the droplets[11], replica symmetry breaking (RSB)[12], and the intermediate Trivial-Non-Trivial (TNT) picture[13].

Droplets expects two equilibrium states related by global spin reversal. The SG order parameter, the spin overlap q , takes only two values $q = \pm q_{EA}$. In the RSB scenario an infinite number of pure states influence the dynamics[12, 14, 15], so that all $-q_{EA} \leq q \leq q_{EA}$ are reachable. TNT[13] describes the SG phase similarly to

an antiferromagnet with random boundary conditions: even if q behaves as for RSB systems, TNT agrees with droplets in the vanishing surface-to-volume ratio of the largest thermally activated spin domains (i.e. the link-overlap defined below takes a single value).

Droplets isothermal aging[16] is that of a disguised ferromagnet[36]. A picture of isothermal aging emerges that applies to basically all coarsening systems: superuniversality[16]. For $T < T_c$ the dynamics consists in the growth of compact domains (inside which the spin overlap coherently takes one of its possible values $q = \pm q_{EA}$). Time dependencies are entirely encoded in the growth law of these domains, $\xi(t)$. The antiferromagnet analogy suggests a similar TNT Aging behavior.

Since in the RSB scenario $q=0$ equilibrium states do exist, the nonequilibrium dynamics starts, and remains forever, with a vanishing order parameter. The replicon, a critical mode analogous to magnons in Heisenberg ferromagnets, is present for all $T < T_c$ [17]. Furthermore, q is not a privileged observable (overlap equivalence[14]): the link overlap displays equivalent Aging behavior.

These theories need numerics to be quantitative[18, 19, 20, 21, 22, 23, 24, 25, 26], but simulations are too short: one Monte Carlo Step (MCS) corresponds to 10^{-12} s[1]. The experimental scale is at 10^{14} MCS (~ 100 s), while typical nonequilibrium simulations reach $\sim 10^{-5}$ s. In fact, high-performance computers have been designed for SG simulations[27, 28, 29].

Here we present the results of a large simulation campaign performed on the application-oriented Janus computer [29]. Janus allows us to simulate the SG instantaneous quench protocol for 10^{11} MCS (~ 0.1 s), enough to reach experimental times by mild extrapolations. Aging is investigated both as a function of time and temper-

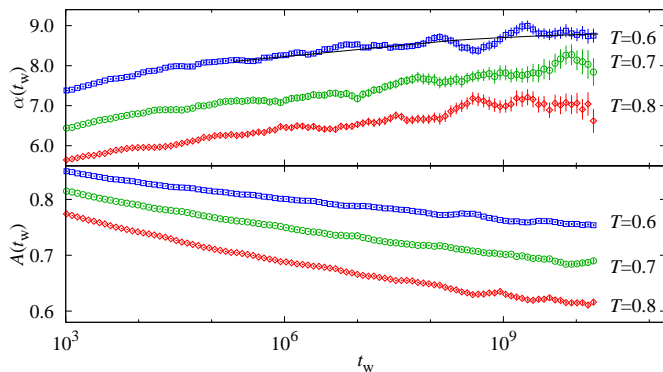


FIG. 1: (Color online) Fit parameters, A and α ($C(t, t_w) = A(t_w)(1 + t/t_w)^{-1/\alpha(t_w)}$) vs. t_w for temperatures below T_c ($T=0.6$ line: fit (for $t_w > 10^5$) to $\alpha(t_w) = \alpha_0 + \alpha_1 \log t_w + \alpha_2 \log^2 t_w$, $\alpha_0 = 6.35795$, $\alpha_1 = 0.18605$, $\alpha_2 = -0.00351835$, diagonal $\chi^2/\text{dof} = 66.26/63$). Coherent oscillations are due to the strong correlations of $\alpha(t_w)$ at neighboring times (neither statistical errors nor the fitting curve nor χ^2/dof vary if one bins data in blocks of 5 consecutive t_w).

ature. We obtain model-independent determinations of the SG coherence length ξ . Conclusive evidence is presented for a critical correlator associated with the replica mode. We observe non trivial Aging in the link correlation (a *nonequilibrium* test of overlap equivalence[14]). We conclude that, up to experimental scales, SG dynamics is not coarsening like.

The $D=3$ Edwards-Anderson Hamiltonian is

$$\mathcal{H} = - \sum_{\langle \mathbf{x}, \mathbf{y} \rangle} J_{\mathbf{x}, \mathbf{y}} \sigma_{\mathbf{x}} \sigma_{\mathbf{y}}, \quad (\langle \dots \rangle : \text{nearest neighbors}). \quad (1)$$

The spins $\sigma_{\mathbf{x}} = \pm 1$ are placed on the nodes, \mathbf{x} , of a cubic lattice of linear size L and periodic boundary conditions. The couplings $J_{\mathbf{x}, \mathbf{y}} = \pm 1$ are chosen randomly with 50% probability, and are quenched variables. For each choice of the couplings (one sample), we simulate two independent systems, $\{\sigma_{\mathbf{x}}^{(1)}\}$ and $\{\sigma_{\mathbf{x}}^{(2)}\}$. We denote by $\overline{(\dots)}$ the average over the couplings. Model (1) undergoes a SG transition at $T_c = 1.101(5)$ [30].

Our $L = 80$ systems evolve with a Heat-Bath dynamics[31], which is in the Universality Class of the physical evolution. The fully disordered starting spin configurations are instantaneously placed at the working temperature (96 samples at $T = 0.8 \approx 0.73 T_c$, 64 at $T = 0.7 \approx 0.64 T_c$ and 96 at $T = 0.6 \approx 0.54 T_c$). We also perform shorter simulations (32 samples) at T_c , as well as $L=40$ and $L=24$ runs to check for Finite-Size effects.

A crucial quantity in non equilibrium dynamics is the two-times correlation function (defined in terms of the field $c_{\mathbf{x}}(t, t_w) \equiv \sigma_{\mathbf{x}}(t + t_w) \sigma_{\mathbf{x}}(t_w)$)[18, 19, 22]:

$$C(t, t_w) = L^{-3} \sum_{\mathbf{x}} \overline{c_{\mathbf{x}}(t, t_w)}, \quad (2)$$

linearly related to the real part of the a.c. susceptibility at waiting time t_w and frequency $\omega = \pi/t$.

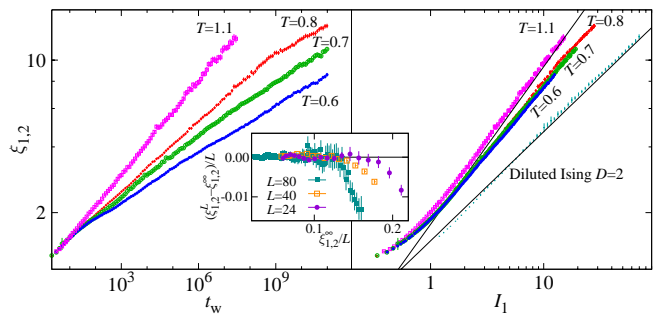


FIG. 2: (Color online) **Left:** SG coherence length $\xi_{1,2}$ vs. waiting time, for $T \leq T_c$. **Right:** $\xi_{1,2}$ vs. I_1 , ($\xi_{1,2} \propto I_1^{1/(2-a)}$). Also shown data for the 2-D site-diluted Ising model ($L = 4096$, 25% dilution, average over 20 samples, $T = 0.64 T_c^{\text{Ising}}$, $\xi_{1,2}$ and I_1 rescaled by 2 for clarity). Full lines correspond to Ising $a=0$, (coarsening) and to the SG, $a(T_c) = 0.616$ [30]. **Inset:** $[\xi_{1,2}^L(t_w) - \xi_{1,2}^\infty(t_w)]/L$ vs. $\xi_{1,2}^\infty(t_w)/L$ for $T=0.8$ and $L=24, 40$ and 80 ($\xi_{1,2}^\infty(t_w)$ from a fit $\xi_{1,2}(t_w) = A(T)t_w^{1/z(T)}$ for $L=80$ in the range $3 < \xi_{1,2} < 10$, see text).

To check for Full-Aging[3] in a systematic way, we fit $C(t, t_w)$ as $A(t_w)(1 + t/t_w)^{-1/\alpha(t_w)}$ in the range $t_w \leq t \leq 10t_w$ [37], obtaining fair fits for all $t_w > 10^3$. To be consistent with the experimental claim of Full-Aging behavior for $10^{14} < t_w < 10^{16}$ [3], $\alpha(t_w)$ should be constant in this t_w range. Although $\alpha(t_w)$ keeps growing for our largest times (with the large errors in[22] it seemed constant for $t_w > 10^4$), its growth slows down. The behavior at $t_w = 10^{16}$ seems beyond reasonable extrapolation.

The coherence length is studied from the correlations of the replica field $q_{\mathbf{x}}(t_w) \equiv \sigma_{\mathbf{x}}^{(1)}(t_w) \sigma_{\mathbf{x}}^{(2)}(t_w)$,

$$C_4(\mathbf{r}, t_w) = L^{-3} \sum_{\mathbf{x}} \overline{q_{\mathbf{x}}(t_w) q_{\mathbf{x}+\mathbf{r}}(t_w)}. \quad (3)$$

For $T < T_c$, it is well described by[12, 20]

$$C_4(\mathbf{r}, t_w) \sim r^{-a} e^{-(r/\xi(t_w))^b}, \quad a \simeq 0.5, \quad b \simeq 1.5. \quad (4)$$

The actual value of a is relevant. For coarsening dynamics $a = 0$, while in a RSB scenario $a > 0$ and $C_4(r, t_w)$ vanishes at long times for fixed $r/\xi(t_w)$. At T_c , the latest estimate is $a = 1 + \eta = 0.616(9)$ [30].

To study a independently of a particular Ansatz as (4) we consider the integrals

$$I_k(t_w) = \int_0^\infty dr r^k C_4(r, t_w), \quad (5)$$

(e.g. the SG susceptibility is $\chi^{\text{SG}}(t_w) = 4\pi I_2(t_w)$). As we assume $L \gg \xi(t_w)$ we safely reduce the upper limit to $L/2$. If a scaling form $C_4(r, t_w) \sim r^{-a} f(r/\xi(t_w))$ is adequate at large r , then $I_k(t_w) \propto [\xi(t_w)]^{k+1-a}$. It follows that $\xi_{k,k+1}(t_w) \equiv I_{k+1}(t_w)/I_k(t_w)$ is proportional to $\xi(t_w)$ and $I_1(t_w) \propto \xi_{k,k+1}^{2-a}$. We find $\xi^{(2)}(t_w) \approx 0.8 \xi_{1,2}(t_w)$, where $\xi^{(2)}$ is the noisy second-moment estimate[9]. Furthermore, for $\xi_{1,2} > 3$, we find $\xi_{0,1}(t_w) \approx 0.46 \xi_{1,2}(t_w)$, and $\xi^{\text{fit}}(t_w) = 1.06 \xi_{1,2}(t_w)$, (ξ^{fit} from a fit to (4) with $a=0.4$).

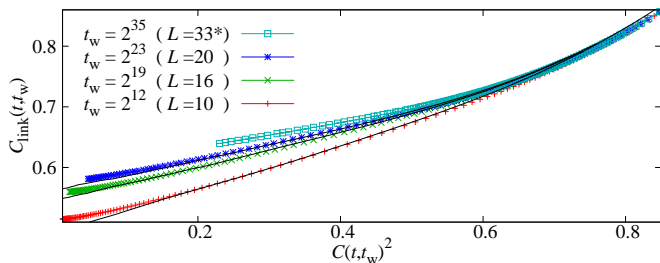


FIG. 3: (Color online) For appropriate t_w and L , the nonequilibrium $C_{\text{link}}(t, t_w)$ vs. $C^2(t, t_w)$ at $T = 0.7$, coincides with equilibrium $Q_{\text{link}}|_q$ vs. q^2 (full lines, data from[34], see text for definitions). The length-time dictionary is $L = 10$ or $t_w = 2^{12}$, $L = 16$ or $t_w = 2^{19}$ and $L = 20$ or $t_w = 2^{23}$. The coherence lengths, $\xi(2^{12}) = 2.75(3)$, $\xi(2^{19}) = 4.23(4)$ and $\xi(2^{23}) = 5.40(7)$, are in the ratio 10:16:20. Hence, from $\xi(2^{35})$, Fig. 2, we predict the equilibrium curve for $L = 33$.

Note that, when $\xi \ll L$, irrelevant distances $r \gg \xi$ largely increase statistical errors for I_k . Fortunately, the very same problem was encountered in the analysis of correlated time series[32], and we may borrow the cure[38].

The largest t_w where $L = 80$ still represents $L = \infty$ physics follows from Finite Size Scaling[31]: for a given numerical accuracy, one should have $L \geq k \xi_{1,2}(t_w)$. To compute k , we compare $\xi_{1,2}^L$ for $L = 24, 40$ and 80 with $\xi_{1,2}^\infty$ estimated with the power law described below (Fig. 2—inset). It is clear that the safe range is $L \geq 7 \xi_{1,2}(t_w)$ at $T = 0.8$ (at T_c the safety bound is $L \geq 6 \xi_{1,2}(t_w)$).

Our results for $\xi_{1,2}$ are shown in Fig. 2. Note for $T = 0.8$ the Finite-Size change of regime at $t_w = 10^9$ ($\xi_{1,2} \sim 11$). We find fair fits to $\xi(t_w) = A(T)t_w^{1/z(T)}$: $z(T_c) = 6.86(16)$, $z(0.8) = 9.42(15)$, $z(0.7) = 11.8(2)$ and $z(0.6) = 14.1(3)$, in good agreement with previous numerical and experimental findings $z(T) = z(T_c)T_c/T$ [5, 20]. We restricted the fitting range to $3 \leq \xi \leq 10$, to avoid both Finite-Size and lattice discretization effects. Extrapolating to experimental times ($t_w = 10^{14} \sim 100$ s), we find $\xi = 14.0(3)$, $21.2(6)$, $37.0(14)$ and $119(9)$ for $T = 0.6$, $T = 0.7$, $T = 0.8$ and $T = 1.1 \approx T_c$, respectively, which seem fairly sensible compared with experimental data[5, 6].

In Fig. 2, we also explore the scaling of I_1 as a function of $\xi_{1,2}$ ($I_1 \propto \xi^{2-a}$). The nonequilibrium data for $T = 1.1$ scales with $a = 0.585(12)$. The deviation from the *equilibrium* estimate $a = 0.616(9)$ [30] is at the limit of statistical significance (if present, it would be due to scaling corrections). For $T = 0.8, 0.7$ and 0.6 , we find $a = 0.442(11)$, $0.355(15)$ and $0.359(13)$ respectively (the residual T dependence is probably due to critical effects still felt at $T = 0.8$). Note that ground state computations for $L \leq 14$ yielded $a(T = 0) \approx 0.4$ [33]. These numbers differ both from critical and coarsening dynamics ($a = 0$).

We finally address the aging properties of $C_{\text{link}}(t, t_w)$

$$C_{\text{link}}(t, t_w) = \overline{\sum_{\langle \mathbf{x}, \mathbf{y} \rangle} c_{\mathbf{x}}(t, t_w) c_{\mathbf{y}}(t, t_w)} / (3L^3). \quad (6)$$

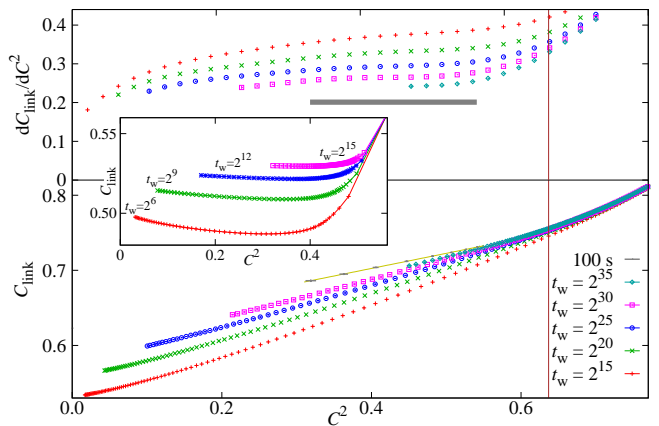


FIG. 4: (Color online) **Bottom:** $C_{\text{link}}(t, t_w)$ vs. $C^2(t, t_w)$ for $T = 0.6$ and some of our largest t_w (vertical line: q_{EA}^2 from[23]). We also show our extrapolation of the C_{link} vs. C^2 curve to $t_w = 10^{14}$ (~ 100 s, see text). **Top:** Derivative of C_{link} with respect to C^2 for $T = 0.6$. The horizontal line corresponds to the slope of a linear fit of $t_w = 10^{14}$ extrapolations (the line width equals twice the error). **Inset:** As in bottom panel, for the ferromagnetic site-diluted $D = 2$ Ising model (same simulation of Fig. 2).

Experimentalists have yet to find a way to access C_{link} , which is complementary to $C(t, t_w)$ (it does not vanish if the configurations at $t + t_w$ and t_w differ by the spin inversion of a compact region of half the system size).

It is illuminating to eliminate t as independent variable in favor of $C^2(t, t_w)$, Figs. 3 and 4. Our expectation for a coarsening dynamics is that, for $C^2 < q_{\text{EA}}^2$ and large t_w , C_{link} will be C -independent (the relevant system excitations are the spin-reversal of compact droplets not affecting C_{link}). Conversely, in a RSB system new states are continuously found as time goes by, so we expect a non constant C^2 dependence even if $C < q_{\text{EA}}$ [39].

General arguments tell us that the nonequilibrium C_{link} at finite *times* coincides with equilibrium correlation functions for systems of finite *size*[10], Fig. 3 (Q_{link} is just $C_4(r = 1)$, while q is the spatial average of $q_{\mathbf{x}}$, Eq.(3)). Therefore, see caption to Fig. 3, we predict the q^2 dependency of the *equilibrium* conditional expectation $Q_{\text{link}}|_q$ for lattices as large as $L = 33$.

As for the shape of the curve $C_{\text{link}} = f(C^2, t_w)$, Fig. 4—bottom, the t_w dependency is residual. Within our time window, C_{link} is not constant for $C < q_{\text{EA}}$. For comparison (inset) we show the, qualitatively different, curves for a coarsening dynamics. Therefore, a major difference between a coarsening and a SG dynamics is in the derivative dC_{link}/dC^2 , for $C^2 < q_{\text{EA}}^2$, Fig. 4—top. We first smooth the curves by fitting $C_{\text{link}} = f(C^2)$ to the lowest order polynomial that provides a fair fit (seventh order for $t_w \leq 2^{25}$, sixth for larger t_w), whose derivative was taken afterwards (Jackknife's statistical errors).

Furthermore, we have extrapolated both $C_{\text{link}}(t = rt_w, t_w)$ and $C(t = rt_w, t_w)$ to $t_w \approx 10^{14}$ (~ 100 s), for

$r=8, 4, \dots, \frac{1}{16}$ [40]. The extrapolated points for $t_w=10^{14}$ fall on a straight line whose slope is plotted in the upper panel (thick line). The derivative is non vanishing for $C^2 < q_{EA}^2$, for the experimental time scale.

In summary, Janus[29] halves the (logarithmic) time-gap between simulations and nonequilibrium Spin Glass experiments. We analyzed the simplest temperature quench, finding numerical evidence for a non-coarsening dynamics, at least up to experimental times (see also[26]). Let us highlight: *nonequilibrium* overlap equivalence (Figs. 3,4); nonequilibrium scaling functions reproducing *equilibrium* conditional expectations in finite systems (Fig. 3); and a nonequilibrium replicon exponent compatible with equilibrium computations[33]. The growth of the coherence length sensibly extrapolates to $t_w = 100$ s (our analysis of dynamic heterogeneities[25, 26] will appear elsewhere[35]). Exploring with Janus nonequilibrium dynamics up to the *seconds* scale will allow the investigation of many intriguing experiments.

We corresponded with M. Hasenbusch, A. Pelissetto and E. Vicari. Janus was supported by EU FEDER funds (UNZA05-33-003, MEC-DGA, Spain), and developed in collaboration with ETHlab. We were partially supported by MEC (Spain), through contracts No. FIS2006-08533, FIS2007-60977, FPA2004-02602, TEC2007-64188; by CAM (Spain) and the Microsoft Prize 2007.

-
- [1] J. A. Mydosh, *Spin Glasses: an Experimental Introduction* (Taylor and Francis, London 1993).
- [2] E. Vincent et al., in *Complex Behavior of Complex Systems*, Lecture Notes in Physics **492**.
- [3] G.F. Rodriguez, G.G. Kenning, and R. Orbach, Phys. Rev. Lett. **91**, 037203 (2003).
- [4] V. Dupuis et al., Pramana J. of Phys. **64**, 1109 (2005).
- [5] Y. G. Joh et al., Phys. Rev. Lett. **82**, 438 (1999).
- [6] F. Bert et al., Phys. Rev. Lett. **92**, 167203 (2004).
- [7] K. Gunnarsson et al., Phys. Rev. B **43**, 8199 (1991).
- [8] M. Palassini and S. Caracciolo, Phys. Rev. Lett. **82**, 5128 (1999).
- [9] H. G. Ballesteros et al., Phys. Rev. B **62**, 14237 (2000).
- [10] S. Franz, M. Mézard, G. Parisi, and L. Peliti, Phys. Rev. Lett. **81**, 1758 (1998); J. Stat. Phys. **97**, 459 (1999).
- [11] W. L. McMillan, J. Phys. C **17**, 3179 (1984); A. J. Bray, M. A. Moore, in *Heidelberg Colloquium on Glassy Dynamics*, Lecture Notes in Physics **275**; J. L. van Hemmen and I. Morgenstern (ed. Springer, Berlin). D. S. Fisher, D. A. Huse, Phys. Rev. Lett. **56**, 1601 (1986) and Phys. Rev. B **38**, 386 (1988).
- [12] E. Marinari et al., J. Stat. Phys. **98**, 973 (2000).
- [13] F. Krzakala and O. C. Martin, Phys. Rev. Lett. **85**, 3013 (2000); M. Palassini and A.P.Young, Phys. Rev. Lett. **85**, 3017 (2000).
- [14] G. Parisi and F. Ricci-Tersenghi, J. Phys. A: Math. Gen. **33**, 113 (2000).
- [15] P. Contucci and C. Giardinà, J. Stat. Phys. **126**, 917 (2007); Ann. Henri Poincaré **6**, 915 (2005).
- [16] D. S. Fisher and D. A. Huse, Phys. Rev. B **38**, 373 (1988).
- [17] C. De Dominicis, I. Kondor, and T. Temesvári, in *Spin Glasses and Random Fields*, edited by P. Young, World Scientific (Singapore 1997).
- [18] J. Kisker, L. Santen, M. Schreckenberg, and H. Rieger, Phys. Rev. B **53**, 6418 (1996).
- [19] H. Rieger, J. Phys. A **26**, L615 (1993).
- [20] E. Marinari, G. Parisi, F. Ricci-Tersenghi, and J. J. Ruiz-Lorenzo, J. Phys. A **33**, 2373 (2000).
- [21] L. Berthier and J.-P. Bouchaud, Phys. Rev. B **66**, 054404 (2002).
- [22] S. Jimenez, V. Martin-Mayor, G. Parisi, and A. Tarancón, J. Phys. A: Math. and Gen. **36**, 10755 (2003).
- [23] S. Perez Gaviro, J.J. Ruiz-Lorenzo, and A. Tarancón, J. Phys. A: Math. Gen. **39** (2006) 8567-8577.
- [24] S. Jimenez, V. Martin-Mayor, and S. Perez-Gaviro, Phys. Rev. B **72**, 054417 (2005).
- [25] L.C. Jaubert, C. Chamon, L.F. Cugliandolo, and M. Picco, J. Stat. Mech. (2007) P05001; H.E. Castillo, C. Chamon, L.F. Cugliandolo, and M.P. Kennett, Phys. Rev. Lett. **88**, 237201 (2002); H.E. Castillo et al., Phys. Rev. B **68**, 134442 (2003).
- [26] C. Aron, C. Chamon, L.F. Cugliandolo, M. Picco, J. Stat. Mech. P05016, (2008).
- [27] A. Cruz et al., Comp. Phys. Comm. **133**, 165 (2001).
- [28] A. Ogielski, Phys. Rev. B **32**, 7384 (1985).
- [29] F. Belletti et al., Computing in Science & Engineering **8**, 41-49 (2006); Comp. Phys. Comm. **178**, 208 (2008); preprint arXiv:0710.3535.
- [30] M. Hasenbusch, A. Pelissetto, and E. Vicari, J. Stat. Mech. L02001 (2008) and private communication.
- [31] See, e.g., D. J. Amit and V. Martin-Mayor, *Field Theory, the Renormalization Group and Critical Phenomena*, (World-Scientific Singapore, third edition, 2005).
- [32] See e.g. A.D. Sokal, in *Functional Integration: Basics and Applications* (1996 Cargèse school), ed. C. DeWitt-Morette, P. Cartier, and A. Folacci (Plenum, N.Y., 1997).
- [33] E. Marinari and G. Parisi, Phys. Rev. Lett. **86**, 3887 (2001).
- [34] P. Contucci et al., Phys. Rev. Lett. **99**, 057206 (2007); P. Contucci, C. Giardinà, C. Giberti, and C. Vernia, Phys. Rev. Lett. **96**, 217204 (2006).
- [35] The Janus collaboration (manuscript in preparation).
- [36] Temperature chaos could spoil the analogy if temperature is varied during the Aging experiment[16].
- [37] Because data at different t and t_w are exceedingly correlated, for all fits in this work we consider the diagonal χ^2 (i.e. we keep only the diagonal terms in the covariance matrix). The effect of time correlations is considered by first forming jackknife blocks[31] (JKB) with the data for different samples (JKB at different t and t_w preserve time correlations), then minimizing χ^2 for each JKB[22].
- [38] We numerically integrate $C_4(r, t_w)$ up to a t_w dependent cutoff, chosen as the smallest integer such that $C_4(r^{\text{cutoff}}(t_w), t_w)$ was smaller than three times its own statistical error. We estimate the (small) remaining contribution, by fitting to Eq.(4) then integrating numerically the fitted function from $r^{\text{cutoff}}-1$ to $L/2$. Details (including consistency checks) will be given elsewhere[35].
- [39] $C_{\text{link}}=C^2$ in the full-RSB Sherrington-Kirkpatrick model.
- [40] For each r , both the link and the spin correlation functions are independently fitted to $a_r + b_r t_w^{-c_r}$ (fits are stable for $t_w > 10^5$ with $c_r \approx 0.5$). These fits are then used to extrapolate the two correlation functions to $t_w = 10^{14}$.